Polymer Journal (2024) 56:505–515
https://doi.org/10.1038/s41428-023-00881-7

ORIGINAL ARTICLE

Variable swelling behavior of and drug encapsulation in a maleimide-modified hyaluronic acid nanogel-based hydrogel

Kohei Yabuuchi[1,2] · Toru Katsumata[2] · Tsuyoshi Shimoboji[2] · Yoshihide Hashimoto[1] · Tsuyoshi Kimura[1] · Kazunari Akiyoshi[3] · Akio Kishida[1]

Received: 29 September 2023 / Revised: 29 November 2023 / Accepted: 4 December 2023 / Published online: 16 January 2024

Abstract

Hyaluronic acid (HA) has garnered much attention in the development of novel hydrogels. Hydrogels, as drug delivery systems, are very important in tissue engineering applications. In this study, we developed a novel HA nanogel containing a cholesterol and maleimide derivative (HAMICH) and its corresponding crosslinked hydrogel (HAMICH gel) to encapsulate drugs for their subsequent release. HAMICH gels self-assemble into nanoparticles via hydrophobic interactions. Dynamic light scattering analysis of HAMICH revealed that the particle size tended to decrease with increasing degree of cholesterol moiety substitution. The HAMICH gel was prepared through a Michael addition reaction between HAMICH and pentaerythritol tetra(mercaptoethyl)polyoxyethylene. The concentration of HAMICH needed for gelation depends on the degree of cholesterol moiety substitution; the higher the substitution degree is, the greater the concentration of HAMICH needed. The HAMICH gel exhibited less swelling and a smaller volume change than the gel with an unmodified cholesterol moiety in phosphate-buffered saline (pH 7.4). The HAMICH gel displayed enhanced peptide and protein trapping abilities without hydrogel swelling, suggesting its potential as a HA hydrogel for biomedical applications.

Introduction

Hydrogels are useful in biomedical applications, such as tissue engineering and drug delivery [1–11]. Numerous hydrogels, including synthetic hydrogels obtained by crosslinking hydrophilic polymers and hydrogels with proteins (e.g., gelatin and collagen) or polysaccharides (e.g., alginic acid and carrageenan) as the main components, have been reported [12–19]. Hyaluronic acid (HA) has attracted considerable attention as a raw polysaccharide. Moreover, as a functional polysaccharide that is a component of the extracellular matrix, HA and its derivatives have been used in various medical applications, including knee, eye, and skin therapy, owing to their biocompatibility and biodegradability [20–28]. For example, HA and its derivatives have been developed for the treatment of osteoarthritis and dry eye [29–31]. In addition, HA interacts with certain proteins, such as aggrecan and tumor necrosis factor-inducible gene 6 protein, as well as receptors, such as CD44, and these interactions are crucial for multiple biological processes, including cell survival, apoptosis, inflammation, and tumorigenesis, suggesting that HA is useful in regenerative medicine and cell therapy. Furthermore, HA is useful as a drug delivery substrate and has various applications [32–39]. Although HA hydrogels have many physiological advantages, they also have several disadvantages, including low mechanical strength due to swelling. In addition, crosslinked hydrogels prepared from

Supplementary information The online version contains supplementary material available at https://doi.org/10.1038/s41428-023-00881-7.

✉ Kazunari Akiyoshi
akiyoshi.kazunari.2e@kyoto-u.ac.jp

✉ Akio Kishida
kishida.mbme@tmd.ac.jp

[1] Institute of Biomaterials and Bioengineering, Tokyo Medical and Dental University, 2-3-10 Kanda-surugadai, Chiyoda-ku, Tokyo 101-0062, Japan

[2] New Product Development Office, R&D Group, Healthcare Materials Division, Life Innovation SBU, Asahi Kasei Corp., Chiyoda-ku, Tokyo 100-0006, Japan

[3] Department of Immunology Graduate School of Medicine, Kyoto University, Yoshida-Konoe-cho, Sakyo-ku, Kyoto 606-8501, Japan

HA modified with crosslinkable functional groups such as methacryl or maleimide cannot encapsulate peptides or proteins. This makes it difficult to apply HA crosslinked hydrogels in regenerative medicine, where bioactive proteins such as growth factors are used.

In this study, we focused on crosslinked hydrogels comprising HA modified with cholesterol derivatives and maleimide crosslinking groups. By adjusting the balance of the hydrophobicity of the cholesterol group and the hydrophilicity of HA, we believe that the amount of encapsulated material could be controlled and that hydrophobic drugs could be encapsulated more efficiently. Cholesterol-bearing HA can be used to form nanogels; therefore, by assembling nanogels into a macrogel, we expect to be able to create novel hydrogels with nanogel characteristics, such as the abilities to encapsulate bioactive substances and perform chaperone functions. For this purpose, we prepared HA nanogels using HA modified with cholesteryl and maleimide groups with the aim of constructing a novel crosslinked hydrogel system through a Michael addition reaction using a poly(ethylene glycol) (PEG) crosslinker with a thiol functional group.

Materials and methods

Materials

HA (average molecular weight = 120 kDa) was purchased from Bloomage Biotechnology Japan Co., Ltd. (Tokyo, Japan). Cation-exchange resin (Dowex® 50WX-8-400) was purchased from Sigma–Aldrich (Tokyo, Japan). Cholesteryl chloroformate, *N*-Boc-1,6-hexanediamine, and *N*-(5-aminopentyl)maleimide hydrochloride were purchased from Tokyo Chemical Industry Co., Ltd. (Tokyo, Japan). Hydrochloride 4-(4,6-dimethoxy-1,3,5-triazin-2-yl)-4-methylmorpholinium chloride (DMT-MM) was purchased from Kokusan Chemical Co., Ltd. (Tokyo, Japan). Dimethyl sulfoxide (DMSO) and NaCl were purchased from FUJIFILM Wako Pure Chemical Co., Ltd. (Osaka, Japan). Dialysis membranes (Spectra/Por, molecular weight cutoff = 12–14 kDa) were purchased from Spectrum Laboratories, Inc. (Rancho Dominguez, CA, USA). Pentaerythritol tetra(mercaptoethyl)polyoxyethylene (4-arm-PEG-SH) (molar weight = 1×10^4 g/mol) was purchased from NOF Corporation (Tokyo, Japan). Other chemicals were commercially available, and all other reagents were used without further purification.

Characterization

^{1}H nuclear magnetic resonance (NMR) measurements were performed using a JEOL JNM-A400 spectrometer (JEOL, Tokyo, Japan) with 0.02 N deuterium chloride (DCl)/d6-DMSO as the solvent.

Synthesis of maleimide group-modified HA nanogels containing cholesterol and a maleimide derivative (HAMICH) (cholesteryl and maleimide group-bearing HA)

HA was modified with cholesterol and maleimide derivatives in solution to create new nanoparticles. Cholesteryl-6-aminohexylcarbamate and HA tetra-n-butylammonium salt (HA-TBA) were prepared as described previously [40]. HA-TBA was obtained by converting HA using a cation-exchange resin and reacting it with *N*-(5-aminopentyl)maleimide hydrochloride using DMT-MM as the condensing agent. HA-TBA was fully dissolved in DMSO (1% w/v), after which *N*-(5-aminopentyl)maleimide in DMSO was added, and the mixture was stirred at 25 °C for 5 min. Subsequently, DMT-MM was added to the mixture, which stirred overnight at room temperature. The feed molar ratio was 100:20:24 [glucuronic acid of HA:DMT-MM:*N*-(5-aminopentyl)maleimide hydrochloride]. Thereafter, cholesteryl-6-aminohexylcarbamate was reacted using a similar procedure. The feed molar ratio was 100:x:1.2x (glucuronic acid of HA:DMT-MM:cholesteryl-6-aminohexylcarbamate, where x = 1.2, 5, 10, 16, 22, 31, and 44). The HA product was purified by dialysis with a 12–14 kDa membrane against DMSO, 0.150 M NaCl, and distilled water. The purified HA solution was filtered through a 0.22-μm membrane filter and then lyophilized until dry. For NMR analysis, HAMICH was dissolved in 0.02 N DCl/DMSO. ^{1}H NMR spectra were obtained using a 400 MHz NMR instrument (JNM-ECS400). The degree of maleimidation was 15%, as determined using ^{1}H NMR.

Size exclusion chromatography coupled with multiangle laser scattering

HA derivatives were analyzed by size exclusion chromatography with multiangle light scattering detection (SEC-MALS; Wyatt Dawn NEON multiangle light scattering detector; Wyatt Technology, Santa Barbara, CA, USA) and refractive index monitoring (Optilab refractive index monitor; Wyatt Technology) using an isocratic high-performance liquid chromatography system (Waters Corporation, Milford, MA, USA). The HA derivatives were diluted to 1.0 mg/mL in SEC-MALS buffer (10 mM phosphate buffer, pH 7.4). Separation was performed in SEC-MALS buffer using a Tosoh G4000SWXL column (Tosoh Bioscience, San Francisco, CA, USA) at a flow rate of 0.5 mL/min. Data analysis was performed using ASTRA software (Wyatt Technology) using the dn/dc values of HA.

Dynamic light scattering (DLS)

DLS analysis was performed using the same solvent as that used for SEC. A HAMICH solution in 10 mM phosphate buffer (pH 7.4) was characterized by DLS using an ELSZ-2000 instrument (Otsuka Electronics, Osaka, Japan). Autocorrelation functions were calculated using the cumulant method. The hydrodynamic diameter of HAMICH was analyzed using the Stokes–Einstein equation.

Inverted vial tests (HAMICH gelation tests)

The gelation ability of HAMICH was determined using vial inversion tests. HAMICH gel was prepared by crosslinking through a Michael addition reaction between the maleimide in HAMICH and the thiol groups in 4-arm-PEG-SH. Briefly, HAMICH and 4-arm-PEG-SH were dissolved separately in 10 mM phosphate buffer, and after both materials had dissolved completely, the two solutions were poured into a vial with cooling to 5 °C and then incubated at 37 °C for 30 min. When the sample showed no flow within 5 min, it was classified as either a gel or a sol.

Preparation of the crosslinked HAMICH gels

HAMICH and 4-arm-PEG-SH were dissolved separately in 10 mM phosphate buffer, and after both materials had dissolved completely, the two solutions were poured into a disk-shaped silicone rubber mold (6 mm diameter and 1 mm depth), which was placed on a polytetrafluoroethylene membrane with cooling to 5 °C. Subsequently, a silicone coverslip was used to cover the mold, which was then incubated at 37 °C for 30 min. After the incubation, the samples were transferred to glass vials. The molar ratio of the maleimide groups in HAMICH to the thiol groups in 4-arm-PEG-SH was 1.1:1.

Water uptake by the hydrogel

HAMICH gels (6 mm in diameter and 1 mm thick) were placed at the bottom of replicate preweighed glass vials ($n = 4$). The initial weights of the vials containing the HAMICH gels were measured. Subsequently, 1 mL of phosphate-buffered saline (PBS) was added, and each mixture was incubated at 37 °C. At 1, 12, and 24 h, the buffer solution from each vial was carefully removed, and the vials were weighed to determine the mass of the swollen hydrogel. Subsequently, fresh PBS was added to replace the removed solution. The masses of the original (W_0) and swollen (W_S) hydrogels were calculated by subtracting the mass of the empty vials from the total mass. The water uptake (Q) of the HAMICH gels was calculated by subtracting the initial mass from the swollen mass using the following equation:

$$Q = W_s - W_0(\mathrm{mg})$$

Protein loading and release

HAMICH gels (6 mm in diameter and 1 mm thick) were prepared as previously described and immersed in PBS. After reaching equilibrium swelling, the HAMICH gels were soaked in 1 mL of fluorescein isothiocyanate (FITC)-labeled insulin (FITC-insulin; 100 μg/mL) in PBS at 37 °C. The fluorescence intensity of the supernatant in the vial (200 μL of solution) was measured at specific time points using a DeNovix DS-11 FX+ Spectrophotometer-Fluorometer (with the "Fluoro Protein" module; DeNovix Inc., Wilmington, DE, USA). Subsequently, the fluorescent samples were returned to their original vials. The loading efficiency of FITC-insulin was estimated from the decrease in fluorescence intensity. The in vitro release of FITC-insulin from the HAMICH gels in the presence of serum was also evaluated. Briefly, HAMICH gels complexed with FITC-insulin (6 mm diameter, 1 mm thick) were immersed in 1 mL of PBS containing 10% fetal bovine serum at 37 °C. Next, 200 μL samples of the supernatant were collected at specific times, and their fluorescence intensity was measured using a DeNovix DS-11 FX+ Spectrophotometer-Fluorometer (with the "Fluoro Protein" module; DeNovix, Inc.). Subsequently, the fluorescent samples were returned to their original vials. All the experiments were performed in triplicate.

Results

Synthesis and characterization of HAMICH

HA with a molecular weight of 120 kDa was used to synthesize HAMICH after tetrabutylammonium HA was prepared in a manner similar to that reported previously [40]. Specifically, HAMICH was synthesized by the condensation of an amine or cholesterol derivative with a maleimide group and the carboxylic acid moiety of HA using DMT-MM (Fig. 1). As a result, a characteristic peak derived from the maleimide group was observed at 6.9 ppm, confirming that the target product, in which a maleimide group was added to HA, was successfully obtained (Fig. 2). This reaction proceeded at a high rate of reaction (>90%) for target cholesterol derivative degrees of substitution ranging from 1–30% (Table 1). To prevent residual unreacted cholesterol hydrochloride remaining, the condensing agent DMT-MM was added at 1.1 eq. relative to cholesterol hydrochloride. The unreacted DMT-MM and its degradation products were removed by dialysis, and the analysis was performed with HAMICH in aqueous solution.

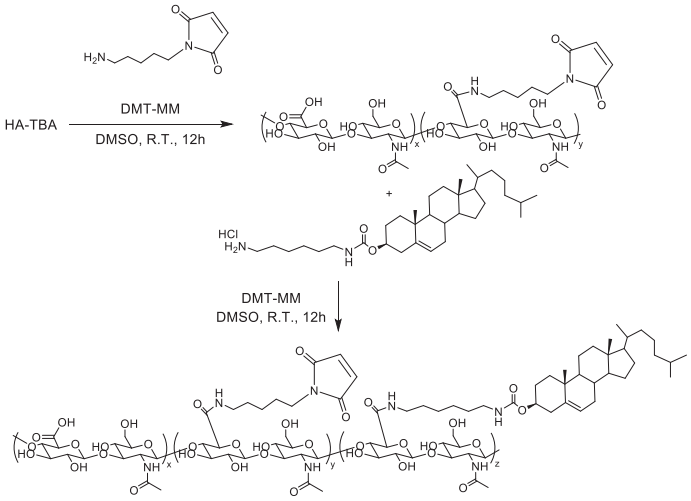

Fig. 1 Scheme for the synthesis of hyaluronic acid (HA) nanogels containing cholesterol and a maleimide derivative (HAMICH)

The absolute molecular weight and number of aggregates in the solution were calculated using a MALS detector. The results showed that the absolute molecular weight increased with increasing degree of cholesterol derivative substitution. Conversely, a decrease in the number of aggregates was observed at a cholesterol derivative substitution degree of 15–20%. Furthermore, at a cholesterol derivative substitution degree of ≥28.6%, the absolute molecular weight increased again, accompanied by an increase in the number of associations.

The size of the particles associated with aggregation in solution was further verified by DLS analysis. When dissolved in 10 mM phosphate buffer (pH 7.4) at a concentration of 2 mg/mL, HAMICH formed nanoparticles by self-aggregating in water, and the smallest particle size was observed for a cholesterol moiety substitution of 20% (Fig. 3).

Crosslinked hydrogel preparation

The gelation behaviors of the maleimide-modified HA derivatives with different degrees of cholesterol derivative substitution were verified by inverted vial tests, and phase diagrams were constructed using the concentrations of the crosslinking agents 4-arm-PEG-SH and HAMICH (Fig. 4a–e). The concentration of HAMICH needed for gelation differed according to the cholesterol incorporation rate; at cholesterol incorporation rates <10%, gelation occurred at HAMICH concentrations <2.5 mg/mL, whereas at cholesterol incorporation rates of 15%, the concentration of HAMICH needed for gelation was >5 mg/mL. Conversely, at a cholesterol incorporation rate of 15%, the concentration needed for gelation was ≥5 mg/mL, and at a cholesterol incorporation rate of 20%, the minimum concentration of HAMICH needed was 10 mg/mL. Gelation was rapid with all cholesterol derivatives, and crosslinked gels formed in at least 30 min.

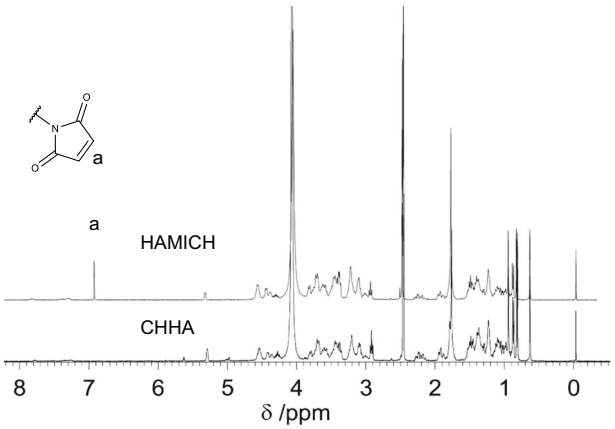

Fig. 2 ^{1}H NMR analysis of HAMICH in 0.02 N DCl/DMSO-d6

Influence of the cholesterol moiety on the water uptake properties

Next, the water uptake behaviors of the crosslinked gels were assessed. Specifically, crosslinked gels were obtained by adjusting the final HAMICH concentration to 7 mg/mL. The resulting gels were immersed in PBS, and water uptake was calculated by tracking the change in weight of the gel. As a result, the water uptake by the HA crosslinked gel without cholesterol (0% Chol) increased by approximately 40% compared to its initial weight. Water uptake by the cholesterol-modified HA-crosslinked gels decreased with increasing cholesterol content. In contrast, water uptake by the cholesterol-unmodified HA-crosslinked gels increased. Additionally, water uptake by the crosslinked gel decreased as the cholesterol content increased (Fig. 5). At all cholesterol incorporation rates, the hydrogels reached equilibrium within 1–3 h of immersion in PBS. A 20% cholesterol incorporation rate was applied with a HAMICH concentration of 16.7 mg/mL because a gel could not be obtained with 7 mg/mL HAMICH (Supplementary Fig. X1).

Table 1 Characteristics of HAMICH

Target degree of Chol moiety [%]	DS[a] [%]	Molecular weight of HAMICH polymer[b] [units, g/mol]	Molecular weight of HAMICH nanoparticle Determined by SEC-MALS [kDa]	Association number of HAMICH [−]
0	0.0	422.42	298.7	2
1	1.3	428.95	853.3	7
5	5.4	448.40	3864.8	29
10	10.3	473.15	9619.1	68
15	14.9	494.77	1947.3	13
20	20.1	520.90	1126.8	7
30	28.6	561.76	3682.4	22

[a]Degree of cholesterol derivative substitution

[b]Molecular weight of the HAMICH polymer calculated using DS. The DS per 100 glucuronic acid units was determined. The DS of the cholesteryl derivative substitution (per 100 HA units) was calculated by the ratio of the integrations of the peak of the N-acetyl group in HA (δ = 1.8, 3H, $COCH_3$) and that of the methyl group in cholesterol (δ = 0.7, 3H, CH_3) in the ^{1}H NMR spectrum. The DS of the maleimide derivative substitution (per 100 HA units) was calculated in the same manner. The average molecular weight of the HAMICH polymer was subsequently calculated by dividing the molecular weight derived from the DS by the number of units

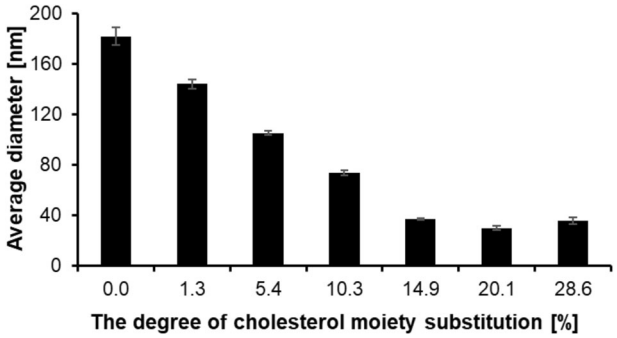

Fig. 3 Characteristics of HAMICH. The results are expressed as the mean ± standard deviation ($n = 3$)

FITC-insulin loading and release

Encapsulation tests were performed using FITC-insulin as a model protein and peptide drug (Fig. 6a). The amount of dye incorporated into the gel was calculated by subtracting the fluorescence intensities of the supernatants. The crosslinked gels with cholesterol showed coloration derived from fluorescent dyes, but the crosslinked gel without cholesterol showed almost no coloration (Fig. 6b). The results showed that crosslinked gels with cholesterol loaded more insulin. Additionally, the highest inclusion amount was observed at a cholesterol incorporation rate of 5–10%, and the amount of encapsulated material was reduced with the 15% HAMICH gel (Fig. 6c). In the cholesterol-unmodified HA-based hydrogel, all of the insulin was released within 1 day. On the other hand, in the cholesterol-modified HA hydrogels, >50% of the insulin was released after 1 day from all the crosslinked gels, and >21 days were needed for the remaining insulin to be released (Fig. 6d).

Discussion

Herein, we report a novel crosslinked HA hydrogel designated HAMICH gel. HAMICH was synthesized by modifying the carboxyl group of glucuronic acid with cholesteryl and maleimide derivatives using HA, which has a relatively low molecular weight (120 kDa) and the advantage of low viscosity compared with that of high-molecular-weight (>500 kDa) HA. Comparison with the 35 kDa molecular weight HA indicated that a lower molecular weight weakens the gel strength; hence, 120 kDa HA was selected (data not shown). In a previous study, dialysis purification was performed under acidic conditions [41]; however, obtaining the target product under neutral conditions was difficult. Under these reaction conditions, the reaction mixture and dialysis mixture were acidic (pH 4–5), and it was presumed that the target product could be obtained stably without degradation of the maleimide group. The pH of the purified aqueous solution before lyophilization was approximately 4. For structural analysis, the unreacted maleimide was removed by dialysis purification, lyophilized, and dissolved in a heavy solvent, and its identity was confirmed by NMR. Cholesteryl HA (CHHA) was synthesized as reported previously [40], and the NMR peaks from samples with and without maleimide were compared for verification. The peak at 6.9 ppm, which is indicative of the maleimide group in HAMICH modified with the maleimide group, was observed, indicating that this group could modify HA (Fig. 2). Additionally, the structures of the synthesized maleimide-modified HA derivatives with different degrees of cholesterol derivative substitution were confirmed by ^{1}H NMR [41].

Next, we analyzed the structure of HAMICH before crosslinking in solution and found that it self-assembles into

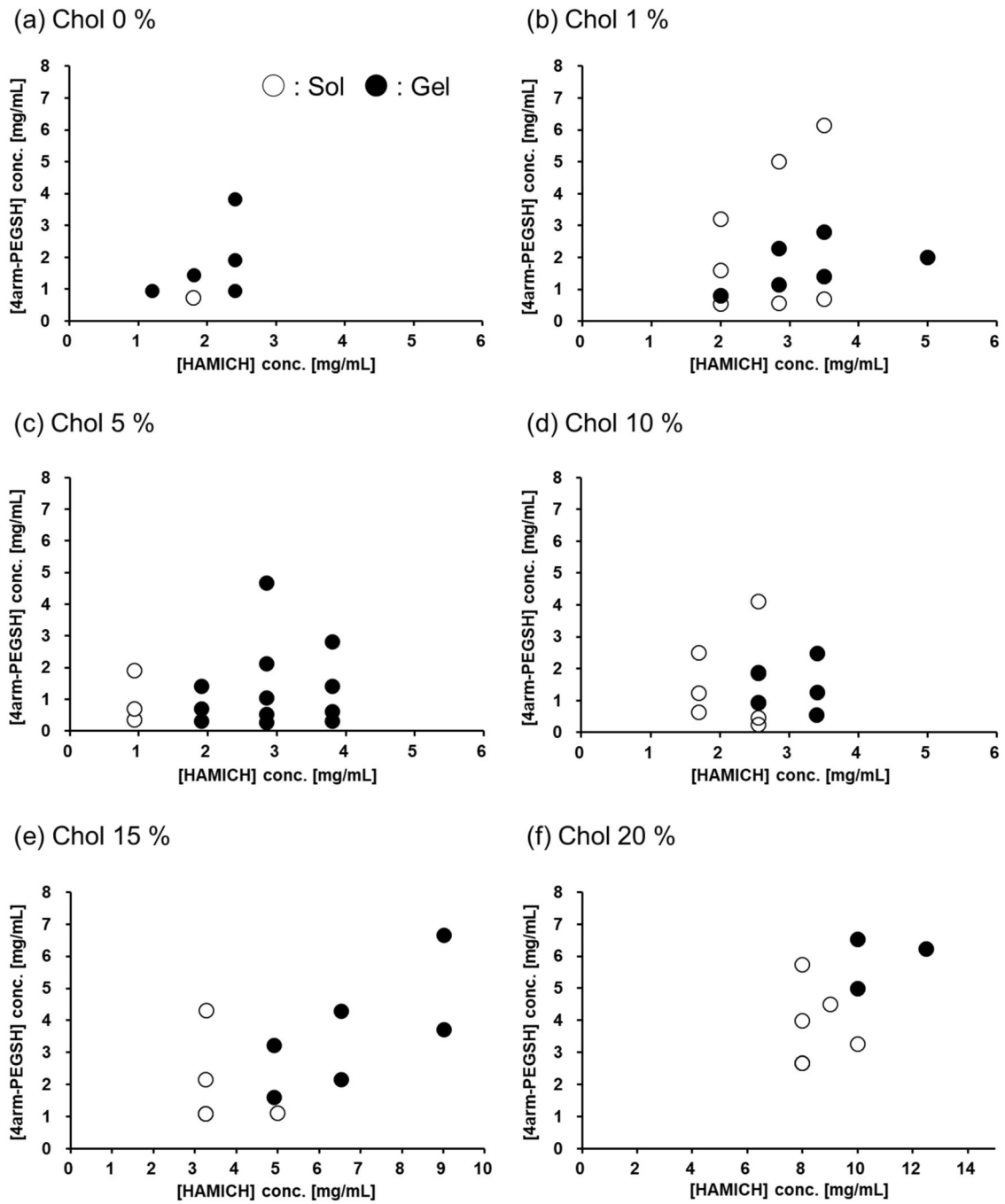

Fig. 4 Phase diagram of the gelation of HAMICH with different degrees of cholesterol moiety substitution

nanoparticles in water via hydrophobic interactions between cholesterol molecules with particle sizes ranging from 10 to 200 nm, depending on the degree of cholesterol moiety substitution. The particle size tended to decrease with increasing cholesterol incorporation. This trend is similar to that observed for conventional cholesteryl-modified HA without the maleimide group. Although the extent of the cholesterol–maleimide interaction is currently unknown, the particle diameter was determined in a cholesterol incorporation rate-dependent manner, suggesting that particles consisting of a core of hydrophobic domains are formed by cholesterol–cholesterol interactions. The distribution of maleimide groups (orientation and position of the functional groups within the nanoparticles), which may be strongly correlated to gelation behavior, should be verified in the future. The smallest particle size was observed with 20% cholesterol incorporation, which tended to differ from that of CHHA nanogels without the maleimide group.

In other words, while the particle size of the previously reported CHHA nanogels was the smallest at a cholesterol incorporation rate of 40%, the particle size of HAMICH increased with a cholesterol incorporation rate of 20%. This suggested that the total carboxy group substitution rate of HA may contribute significantly to the particle size. This difference may be due to a decrease in hydrophilicity resulting from the loss of the carboxylic acid moiety of HA. MALS analysis from a previous report on CHHA nanogels without maleimide also revealed that the particle size decreased and the number of aggregates increased as the degree of cholesterol derivative substitution increased to approximately 40%, indicating a different trend [40].

Next, the gelation behavior of HAMICH, which can form crosslinked gels through a Michael addition reaction between the maleimide and PEGSH mercapto groups, was examined (Fig. 7). Regarding the crosslinking gelation rate, after mixing at a maleimide:thiol (SH) molar ratio of 1.1:1.0, gelation occurred within a few seconds under various specific conditions, suggesting its applicability as a novel in situ gelation system capable of encapsulating proteins. For example, attenuated total reflectance–Fourier transform infrared analysis of the formation of crosslinked hydrogels using HAMICH with 5% cholesteryl modification revealed that the peak at 690 cm^{-1} derived from maleimide disappeared after gelation [42]. Concerning the relationship between the concentrations of the crosslinker groups in 4-arm-PEG-SH and HAMICH, data with cholesterol incorporation rates of 1, 10, and 15% suggest an appropriate range of maleimide:thiol (SH) molar ratios. In other words, by converting the phase diagram into molar ratios, a maleimide:thiol (SH) molar ratio of 1:1 to 2:1 was expected to be the preferred range. This is because at higher concentrations of 4-arm-PEG-SH, the maleimide group may react with the thiol group on one arm of 4-arm-PEG-SH before the intramolecular crosslinking reaction between the

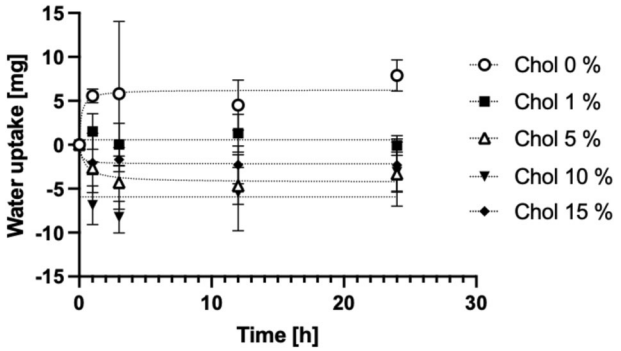

Fig. 5 Water uptake by the HAMICH gel. The results are expressed as the mean ± standard deviation ($n = 4$)

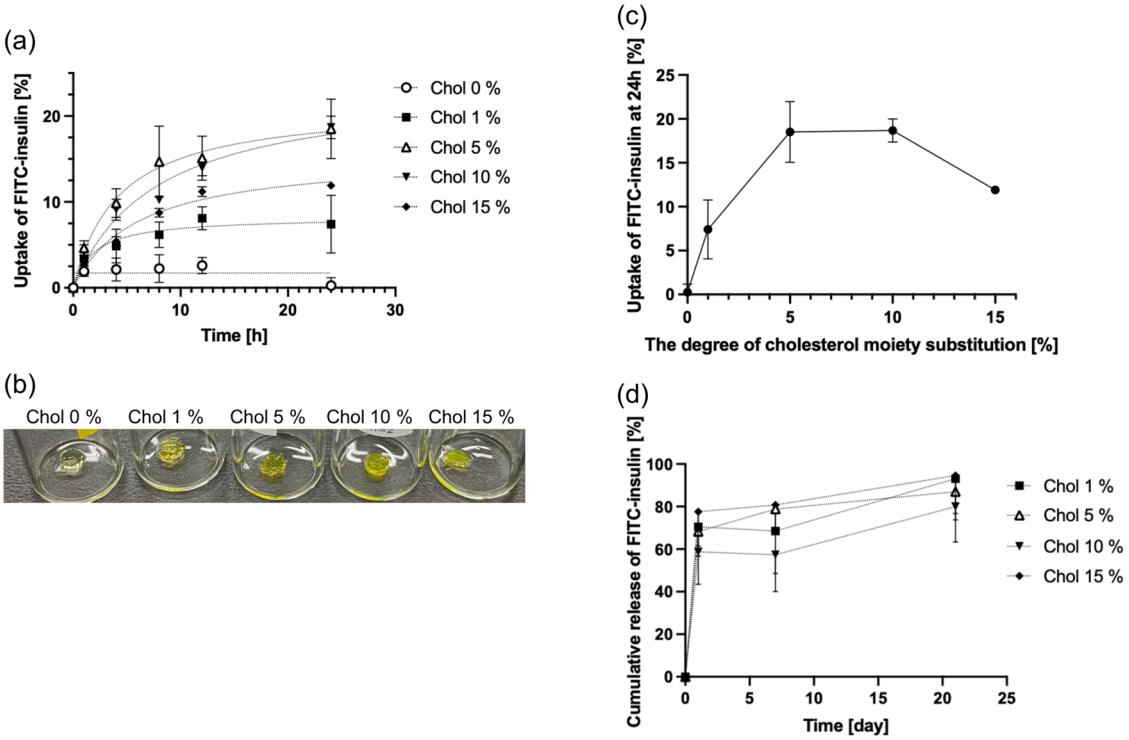

Fig. 6 Insulin encapsulation profiles of the HAMICH gel. **a** Encapsulation of fluorescein isothiocyanate (FITC)-labeled insulin in the HAMICH gel, in which the concentration of HAMICH was 7.0 mg/mL ($n = 3$). **b** Images of hydrogels containing FITC-labeled insulin. **c** Correlation diagram between the degree of cholesterol moiety substitution and the uptake of FITC-labeled insulin at 24 h ($n = 4$). **d** In vitro release of FITC-labeled insulin from HAMICH gels, in which the concentration of HAMICH was 7.0 mg/mL ($n = 3$). The results are expressed as the mean ± standard deviation

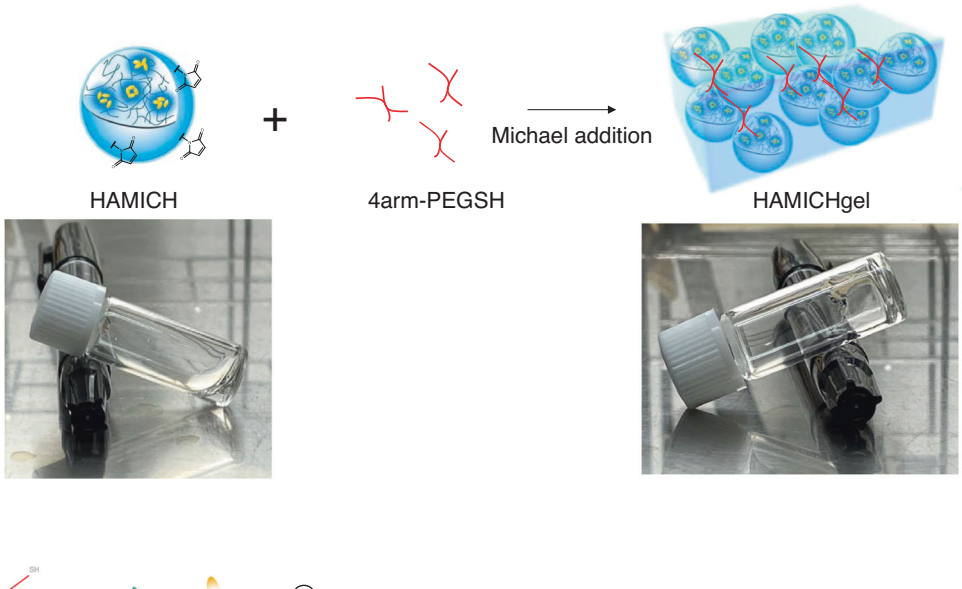

Fig. 7 Schematic illustration of the Michael addition reaction between HAMICH and PEGSH

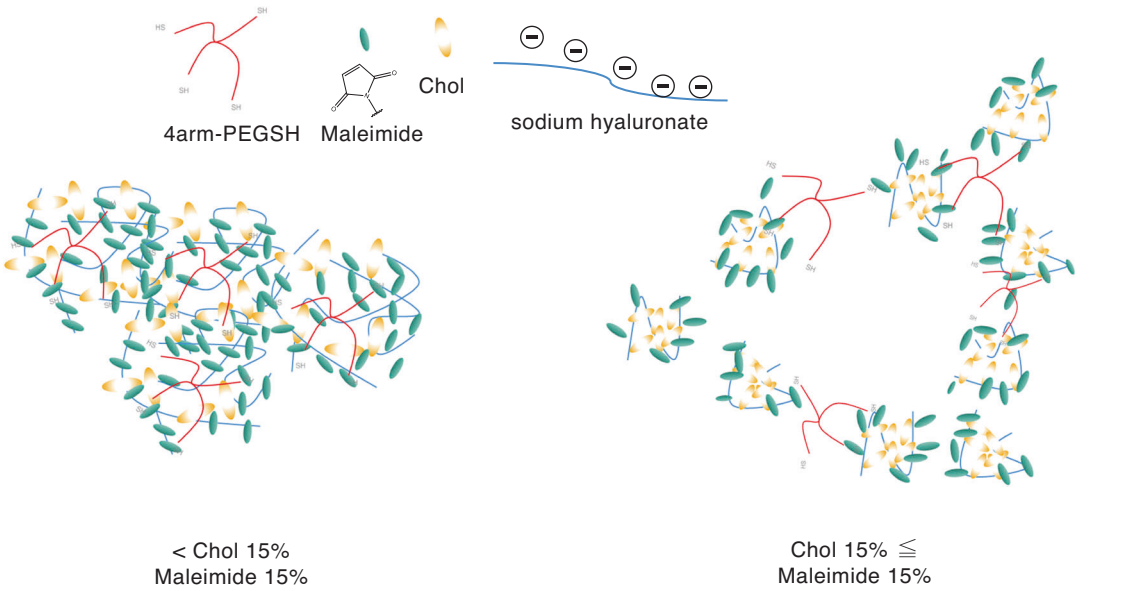

Fig. 8 Schematic illustration of the gelation of HAMICH with 4-arm-PEG-SH

two arms of 4-arm-PEG-SH occurs. Considering the relationship between the cholesterol incorporation rate and HA concentration needed for gelation, gelation occurred even at a very low HA concentration of 3 mg/mL when the cholesterol incorporation rate was <10% with an average particle size was ≥50 nm, as determined by DLS. Conversely, a higher HAMICH concentration (≥4.9 mg/mL) was needed when the cholesterol incorporation ratio was ≥15%. This was due to differences in inter- or intramolecular cholesterol interactions during the self-assembly of the nanoparticles and the fact that the polymer chains do not overlap, making gelation difficult (Fig. 8). In contrast, in a previous study on nanoparticle-based crosslinked hydrogels (cholesterol-bearing pullulan [CHP] crosslinked nanogels), which belong to the same polysaccharide family as HA, a CHP concentration of ≥20 mg/mL was needed to obtain a crosslinked gel [43–45]. This difference may be attributed to the significant difference in the spreading of the polymer chains of pullulan, a nonionic polysaccharide, and HA, a polyelectrolyte, in water. Conversely, we also verified the differences in the crosslinking groups. In other words, we examined crosslinking groups other than maleimide that are amenable to Michael addition. Specifically, we synthesized HA derivatives modified with 3% cholesterol and 20% methacryl groups and crosslinking groups, such as 19% cholesterol and 20% methacryl groups, and examined the possibility of gelation. However, obtaining gels under the same conditions as those of maleimide, even at a

concentration of 20 mg/mL of the HA derivative, was difficult (data not shown). This was due to the low reactivity for the Michael addition reaction, suggesting that the reactivity of the crosslinking group is important for obtaining crosslinked gels consisting of nanoparticles. A more detailed rheological analysis of the relationship between the polymer overlap concentration (C*) and gelation can provide a better understanding of the gelation mechanism [46].

The change in weight (volume) of the gels in PBS was examined. Generally, HA and HA-crosslinked gels are predisposed to extreme swelling owing to their hydrophilic and water-holding properties [47–49]. Water uptake by the cholesterol-unmodified HA-crosslinked gels increased the weight of the gel by approximately 40% compared to its initial weight. This swelling ratio is comparable to that of hydrogels composed of maleimide-modified HA and gelatin reported previously [41]. Conventional cholesterol-unmodified HA hydrogels absorb a considerable amount of water; however, the novel HAMICH hydrogels exhibit less swelling and smaller volume changes. The swelling of crosslinked hydrogels consisting of a novel HA with maleimide and cholesteryl groups could be controlled by the degree of cholesterol substitution. The hydrophobic domain of the HA-crosslinked hydrogel, which participates in hydrophobic interactions between the cholesterol groups, contributes to the suppression of gel swelling.

Finally, insulin was used as a model compound for peptide and protein drugs [50]. On the one hand, in the HA crosslinked gel without cholesterol, almost no insulin was encapsulated because of electrostatic repulsion. On the other hand, in the HA crosslinked gel modified with cholesterol, the insulin inclusion amount increased due to hydrophobic interactions and the relaxation of electrostatic repulsion attributed to the isoelectric point of insulin [50]. The higher the cholesterol incorporation rate (up to 15%), the greater the hydrophobicity and the less drug incorporated. This finding suggested an optimal inclusion range for the degree of cholesterol substitution in cholesteryl-substituted HA nanogels without maleimide modification (Fig. 6c). Although >60% insulin release was observed within 1 d, the release was confirmed to be sustained over an extended period compared with that in the cholesterol-unmodified hydrogel (Fig. 6d). Conventional cholesterol-unmodified HA-based hydrogels do not exhibit cholesterol-driven encapsulation; therefore, encapsulating large amounts of these materials and achieving sustained release are challenging. This method may also be suitable for use with water insoluble drugs. These results suggest that this material may be useful as a novel HA-based hydrogel for loading various drugs. At present, the novel crosslinked HAMICH gel has not undergone biological evaluation. Detailed biological assessments are essential for demonstrating the utility of this biomaterial. Further studies will encompass biological evaluations to understand the biocompatibility of this material and, consequently, to develop the most suitable biomaterial.

Conclusion

In this study, we report a novel crosslinked hydrogel composed of HA modified with cholesteryl, maleimide groups and PEGSH. Gelation depended on the concentrations of HAMICH and PEGSH; however, the needed concentration varied depending on the rate of cholesterol incorporation, with low concentrations enabling crosslinking. Furthermore, the crosslinked hydrogels and nanogels contained a hydrophobic domain derived from cholesterol that inhibited swelling, suggesting that the change in volume could be controlled. These results indicate that the novel crosslinked HA hydrogel, which can encapsulate peptides and proteins and has controllable swelling properties, can be applied in regenerative medicine to control cell differentiation.

Acknowledgements We would like to thank Editage (www.editage.com) for English language editing.

Author contributions Conceptualization: KY, ToK, and KA; Methodology: KY, ToK, TS, YH, TtK, and AK; Validation: KY; Investigation: KY; Writing—Original Draft Preparation: KY; Writing—Review and Editing: TtK, TS, KA, and AK; Project Administration: TS, KA, and AK; and Funding Acquisition: TS, KA, and AK. All the authors have read and agreed to the published version of the manuscript.

Funding KA received a research grant from Asahi Kasei Corp.

Compliance with ethical standards

Conflict of interest KY, ToK, and TS are employees of Asahi Kasei Corp., and KA received a research grant from Asahi Kasei Corp. The other authors declare no conflicts of interest.

Publisher's note Springer Nature remains neutral with regard to jurisdictional claims in published maps and institutional affiliations.

References

1. Langer R, Tirrell DA. Designing materials for biology and medicine. Nature. 2004;428:487–92.
2. Catoira MC, Fusaro L, Di Francesco D, Ramella M, Boccafoschi F. Overview of natural hydrogels for regenerative medicine applications. J Mater Sci Mater Med. 2019;30:115. https://link.springer.com/article/10.1007/s10856-019-6318-7.
3. Ilić-Stojanović S, Nikolić L, Cakić S. A review of patents and innovative biopolymer-based hydrogels. Gels. 2023;9:556. https://www.ncbi.nlm.nih.gov/pubmed/37504436.
4. Munoz-robles BG, Kopyeva I, Deforest CA. Surface patterning of hydrogel biomaterials to probe and direct cell–matrix interactions. Adv Mater Inter. 2020;7:2001198 https://onlinelibrary.wiley.com/doi/abs/10.1002/admi.202001198.
5. Kopeček J, Yang J. Hydrogels as smart biomaterials. Polym Int. 2007;56:1078–98. https://api.istex.fr/ark:/67375/WNG-MM01ZW50-M/fulltext.pdf.
6. Haque MA, Kurokawa T, Gong JP. Super tough double network hydrogels and their application as biomaterials. Polymer. 2012;53:1805–22. https://www.sciencedirect.com/science/article/pii/S0032386112002212.
7. Du X, Zhou J, Shi J, Xu B. Supramolecular hydrogelators and hydrogels: from soft matter to molecular biomaterials. Chem Rev. 2015;115:13165–307. https://pubs.acs.org/doi/10.1021/acs.chemrev.5b00299.
8. Khademhosseini A, Langer R. Microengineered hydrogels for tissue engineering. Biomaterials. 2007;28:5087–92. https://www.clinicalkey.es/playcontent/1-s2.0-S0142961207005480.
9. Caliari SR, Burdick JA. A practical guide to hydrogels for cell culture. Nat Methods. 2016;13:405–14. https://www.ncbi.nlm.nih.gov/pubmed/27123816.
10. Wang RM, Christman KL. Decellularized myocardial matrix hydrogels: in basic research and preclinical studies. Adv Drug Deliv Rev. 2016;96:77–82. https://www.sciencedirect.com/science/article/abs/pii/S0169409X15001143.
11. Lee KY, Mooney DJ. Hydrogels for tissue engineering. Chem Rev. 2001;101:1869–79. https://pubs.acs.org/doi/10.1021/cr000108x.
12. Prabaharan M, Mano JF. Stimuli-responsive hydrogels based on polysaccharides incorporated with thermo-responsive polymers as novel biomaterials. Macromol Biosci. 2006;6:991–1008. https://onlinelibrary.wiley.com/doi/abs/10.1002/mabi.200600164.
13. Almeida HV, Eswaramoorthy R, Cunniffe GM, Buckley CT, O'Brien FJ, Kelly DJ. Fibrin hydrogels functionalized with cartilage extracellular matrix and incorporating freshly isolated stromal cells as an injectable for cartilage regeneration. Acta Biomater. 2016;36:55–62. https://www.sciencedirect.com/science/article/abs/pii/S1742706116300927.
14. Mousavi S, Khoshfetrat AB, Khatami N, Ahmadian M, Rahbarghazi R. Comparative study of collagen and gelatin in chitosan-based hydrogels for effective wound dressing: physical properties and fibroblastic cell behavior. Biochem Biophys Res Commun. 2019;518:625–31. https://www.sciencedirect.com/science/article/abs/pii/S0006291X19316250.
15. Demir GC, Erdemli Ö, Keskin D, Tezcaner A. Xanthan-gelatin and xanthan-gelatin-keratin wound dressings for local delivery of vitamin C. Int J Pharm. 2022;614:121436. https://www.sciencedirect.com/science/article/abs/pii/S0378517321012424.
16. Zhai X, Wu Y, Tan H. Gelatin-based targeted delivery systems for tissue engineering. Curr Drug Targets. 2023;24:673–87. https://www.eurekaselect.com/article/132301.
17. Mahmood A, Patel D, Hickson B, DesRochers J, Hu X. Recent progress in biopolymer-based hydrogel materials for biomedical applications. Int J Mol Sci. 2022;23:1415 https://www.mdpi.com/1422-0067/23/3/1415.
18. Sakai S, Yamaguchi S, Takei T, Kawakami K. Oxidized alginate-cross-linked alginate/gelatin hydrogel fibers for fabricating tubular constructs with layered smooth muscle cells and endothelial cells in collagen gels. Biomacromolecules. 2008;9:2036–41. https://pubs.acs.org/doi/abs/10.1021/bm800286v.
19. Yegappan R, Selvaprithiviraj V, Amirthalingam S, Jayakumar R. Carrageenan based hydrogels for drug delivery, tissue engineering and wound healing. Carbohydr Polym. 2018;198:385–400. https://www.sciencedirect.com/science/article/abs/pii/S0144861718307410.
20. Burdick JA, Chung C, Jia X, Randolph MA, Langer R. Controlled degradation and mechanical behavior of photopolymerized hyaluronic acid networks. Biomacromolecules. 2005;6:386–91. https://pubs.acs.org/doi/abs/10.1021/bm049508a.
21. Burdick JA, Prestwich GD. Hyaluronic acid hydrogels for biomedical applications. Adv Mater. 2011;23:H41–H56. https://api.istex.fr/ark:/67375/WNG-24C3B9RG-6/fulltext.pdf.
22. Schuurmans CCL, Mihajlovic M, Hiemstra C, Ito K, Hennink WE, Vermonden T. Hyaluronic acid and chondroitin sulfate (meth)acrylate-based hydrogels for tissue engineering: synthesis, characteristics and pre-clinical evaluation. Biomaterials. 2021;268:120602 https://www.sciencedirect.com/science/article/pii/S0142961220308486.
23. Xu Q, Torres JE, Hakim M, Babiak PM, Pal P, Battistoni CM, et al. Collagen- and hyaluronic acid-based hydrogels and their biomedical applications. Mater Sci Eng R Rep. 2021;146:100641 https://www.sciencedirect.com/science/article/abs/pii/S0927796X2100036X.
24. Escobar Ivirico JL, Bhattacharjee M, Kuyinu E, Nair LS, Laurencin CT. Regenerative engineering for knee osteoarthritis treatment: biomaterials and cell-based technologies. Engineering (Beijing). 2017;3:16–27. http://lib.cqvip.com/qk/87553B/201701/671470455.html.
25. Jin R, Moreira Teixeira LS, Krouwels A, Dijkstra PJ, van Blitterswijk CA, Karperien M, et al. Synthesis and characterization of hyaluronic acid–poly(ethylene glycol) hydrogels via Michael addition: an injectable biomaterial for cartilage repair. Acta Biomater. 2010;6:1968–77. https://www.sciencedirect.com/science/article/abs/pii/S1742706109005650.
26. Hussain Z, Ei Thu HE, Katas H, Bukhari SNA. Hyaluronic acid-based biomaterials: a versatile and smart approach to tissue regeneration and treating traumatic, surgical, and chronic wounds. Polym Rev. 2017;57:594–630. https://www.tandfonline.com/doi/abs/10.1080/15583724.2017.1315433.
27. Lai JY, Ma DH-K, Cheng HY, Sun CC, Huang SJ, Li YT, et al. Ocular biocompatibility of carbodiimide cross-linked hyaluronic acid hydrogels for cell sheet delivery carriers. J Biomater Sci Polym Ed. 2010;21:359–76. https://www.tandfonline.com/doi/epdf/10.1163/156856209X416980?needAccess=true.
28. Raia NR, Jia D, Ghezzi CE, Muthukumar M, Kaplan DL. Characterization of silk-hyaluronic acid composite hydrogels towards vitreous humor substitutes. Biomaterials. 2020;233:119729. https://www.sciencedirect.com/science/article/abs/pii/S0142961219308476.
29. Kobayashi Y, Okamoto A, Nishinari K. Viscoelasticity of hyaluronic acid with different molecular weights. Biorheology. 1994;31:235–44. https://content.iospress.com/articles/biorheology/bir31-3-02.
30. Sun SF, Chou YJ, Hsu CW, Hwang CW, Hsu PT, Wang JL, et al. Efficacy of intra-articular hyaluronic acid in patients with osteoarthritis of the ankle: a prospective study. Osteoarthritis Cartilage. 2006;14:867–74. https://www.sciencedirect.com/science/article/pii/S1063458406000495.

31. Mohamed YH, Uematsu M, Ueki R, Inoue D, Sasaki H, Kitaoka T. Safety of sodium hyaluronate eye drop with C12-benzalkonium chloride. Cutan Ocul Toxicol. 2019;38:156–60. https://www.tandfonline.com/doi/abs/10.1080/15569527.2018.1543316?journalCode=icot20.
32. Turley EA, Noble PW, Bourguignon LYW. Signaling properties of hyaluronan receptors. J Biol Chem. 2002;277:4589–92. https://www.ncbi.nlm.nih.gov/pubmed/11717317.
33. Lin H, Beck AM, Shimomura K, Sohn J, Fritch MR, Deng Y, et al. Optimization of photocrosslinked gelatin/hyaluronic acid hybrid scaffold for the repair of cartilage defect. J Tissue Eng Regen Med. 2019;13:1418–29. https://onlinelibrary.wiley.com/doi/abs/10.1002/term.2883.
34. Tan H, Li H, Rubin JP, Marra KG. Controlled gelation and degradation rates of injectable hyaluronic acid-based hydrogels through a double crosslinking strategy. J Tissue Eng Regen Med. 2011;5:790–7. https://api.istex.fr/ark:/67375/WNG-8W6F50MM-4/fulltext.pdf.
35. Poldervaart MT, Goversen B, de Ruijter M, Abbadessa A, Melchels FPW, Öner FC, et al. 3D bioprinting of methacrylated hyaluronic acid (MeHA) hydrogel with intrinsic osteogenicity. PLoS One. 2017;12:e0177628 https://journals.plos.org/plosone/article?id=10.1371/journal.pone.0177628.
36. Huang G, Huang H. Application of hyaluronic acid as carriers in drug delivery. Drug Deliv. 2018;25:766–72. https://www.tandfonline.com/doi/abs/10.1080/10717544.2018.1450910.
37. Leach JB, Schmidt CE. Characterization of protein release from photocrosslinkable hyaluronic acid-polyethylene glycol hydrogel tissue engineering scaffolds. Biomaterials. 2005;26:125–35. https://www.sciencedirect.com/science/article/abs/pii/S0142961204001565.
38. Shin J, Lee JS, Lee C, Park H, Yang K, Jin Y, et al. Tissue adhesive catechol-modified hyaluronic acid hydrogel for effective, minimally invasive cell therapy. Adv Funct Materials. 2015;25:3814–24. https://api.istex.fr/ark:/67375/WNG-9FCZ6F51-W/fulltext.pdf.
39. Lee KB, Hui JH, Song IC, Ardany L, Lee EH. Injectable mesenchymal stem cell therapy for large cartilage defects—A porcine model. Stem Cells (Dayt Ohio). 2007;25:2964–71. https://onlinelibrary.wiley.com/doi/abs/10.1634/stemcells.2006-0311.
40. Nakai T, Hirakura T, Sakurai Y, Shimoboji T, Ishigai M, Akiyoshi K. Injectable hydrogel for sustained protein release by salt-induced association of hyaluronic acid nanogel. Macromol Biosci. 2012;12:475–83. https://api.istex.fr/ark:/67375/WNG-HF5MTP24-K/fulltext.pdf.
41. Yoo KM, Murphy SV, Skardal A. A rapid crosslinkable maleimide-modified hyaluronic acid and gelatin hydrogel delivery system for regenerative applications. Gels. 2021;7:13 https://www.mdpi.com/2310-2861/7/1/13.
42. Yabuuchi K, Suzuki M, Liang C, Hashimoto Y, Kimura T, Akiyoshi K. et al. Preparation of cholesterol-modified hyaluronic acid nanogel-based hydrogel and the inflammatory evaluation using macrophage-like cells. Gels. 2023;9:866. https://doi.org/10.3390/gels9110866.
43. Hashimoto Y, Mukai SA, Sawada S, Sasaki Y, Akiyoshi K. Nanogel tectonic porous gel loading biologics, nanocarriers, and cells for advanced scaffold. Biomaterials. 2015;37:107–15. https://www.clinicalkey.es/playcontent/1-s2.0-S0142961214010941.
44. Kinoshita N, Sasaki Y, Marukawa E, Hirose R, Sawada SI, Harada H, et al. Crosslinked nanogel-based porous hydrogel as a functional scaffold for tongue muscle regeneration. J Biomater Sci Polym Ed. 2020;31:1254–71. https://www.tandfonline.com/doi/abs/10.1080/09205063.2020.1744246.
45. Tahara Y, Kosuge S, Sawada S-i, Sasaki Y, Akiyoshi K. Nanogel bottom-up gel biomaterials for protein delivery: photopolymerization of an acryloyl-modified polysaccharide nanogel macromonomer. Reactive and Functional Polymers. 2013;73:958–64. https://www.sciencedirect.com/science/article/abs/pii/S138151481300031X.
46. Liu W, Gong X, Zhu Y, Wang J, Ngai T, Wu C. Probing sol–gel matrices and dynamics of star PEG hydrogels near overlap concentration. Macromolecules. 2019;52:8956–66. https://pubs.acs.org/doi/abs/10.1021/acs.macromol.9b01489.
47. Zawko SA, Suri S, Truong Q, Schmidt CE. Photopatterned anisotropic swelling of dual-crosslinked hyaluronic acid hydrogels. Acta Biomater. 2009;5:14–22. https://www.sciencedirect.com/science/article/abs/pii/S1742706108002869.
48. Zhao Y, Yi B, Hu J, Zhang D, Li G, Lu Y, et al. Double Cross-linked biomimetic hyaluronic acid-based hydrogels with thermo-stimulated self-contraction and tissue adhesiveness for accelerating post-wound closure and wound healing. Adv Funct Materials. 2023;33:2300710. https://onlinelibrary.wiley.com/doi/abs/10.1002/adfm.202300710.
49. Albersdörfer A, Sackmann E. Swelling behavior and viscoelasticity of ultrathin grafted hyaluronic acid films. Eur Phys J B. 1999;10:663–72. https://link.springer.com/article/10.1007/s100510050898.
50. Herring R, Russell-Jones DDL. Lessons for modern insulin development. Diabet Med. 2018;35:1320–8. https://onlinelibrary.wiley.com/doi/abs/10.1111/dme.13692.